Sub-cycle QAM modulation for VCSEL-based optical fiber links

Pham, Tien-Thang; Rodes Lopez, Roberto; Jensen, Jesper Bevensee; Chang-Hasnain, Connie J.; Tafur Monroy, Idelfonso

Published in:
Optics Express

Link to article, DOI:
10.1364/OE.21.001830

Publication date:
2013

Document Version
Publisher's PDF, also known as Version of record

Sub-cycle QAM modulation for VCSEL-based optical fiber links

Tien-Thang Pham,[1,*] Roberto Rodes,[1] Jesper Bevensee Jensen,[1] Connie J. Chang-Hasnain,[2] and Idelfonso Tafur Monroy[1]

[1]*DTU Fotonik, Department of Photonics Engineering, Technical University of Denmark, DK2800 Kgs. Lyngby, Denmark*

[2]*Dept. of Electrical Engineering and Computer Science, University of California, Berkeley, CA 94720, USA*

[*]*ptit@fotonik.dtu.dk*

Abstract: QAM modulation utilizing subcarrier frequency lower than the symbol rate is both theoretically and experimentally investigated. High spectral efficiency and concentration of power in low frequencies make sub-cycle QAM signals attractive for optical fiber links with direct modulated light sources. Real-time generated 10-Gbps 4-level QAM signal in a 7.5-GHz bandwidth utilizing subcarrier frequency at a half symbol rate was successfully transmitted over 20-km SMF using an un-cooled 1.5-μm VCSEL. Only 2.5-dB fiber transmission power penalty was observed with no equalization applied.

OCIS codes: (060.2330) Fiber optics communications; (060.4080) Modulation.

References and links

1. W. Hofmann, M. Müller, P. Wolf, A. Mutig, T. Gründl, G. Böhm, D. Bimberg, and M.-C. Amann, "40 Gbit/s modulation of 1550 nm VCSEL," Electron. Lett. **47**(4), 270–271 (2011).
2. P. Moser, W. Hofmann, P. Wolf, G. Fiol, J. A. Lott, N. N. Ledentsov, and D. Bimberg, "83 fJ/bit energy-to-data ratio of 850-nm VCSEL at 17 Gb/s," in *Proceedings of 37th European Conference on Optical Communication* (2011), pp. 1–3.
3. W. Hofmann, M. Görblich, G. Böhm, M. Ortsiefer, L. Xie, and M.-C. Amann, "Long-wavelength 2-D VCSEL arrays for optical interconnects," in *Proceedings of Lasers and Electro-Optics (CLEO) and Quantum Electronics and Laser Science Conference* (2008), pp.1- 2.
4. M. C. Y. Huang, K. B. Cheng, Y. Zhou, A. Pisano, and C. Chang-Hasnain, "Monolithic integrated piezoelectric MEMS-tunable VCSEL," IEEE IEEE J. Sel. Topics Quantum Electron. **13**(2), 374–380 (2007).
5. B. Zhang, X. Zhao, L. Christen, D. Parekh, W. Hofmann, M. C. Wu, M. C. Amann, C. J. Chang-Hasnain, and A. E. Willner, "Adjustable chirp injection-locked 1.55-μm VCSELs for enhanced chromatic dispersion compensation at 10-Gbit/s," in *Optical Fiber Communication Conference* (Optical Society of America, 2008) paper OWT7.
6. L. Xu, H. K. Tsang, W. Hofmann, and M.-C. Amann, "10-Gb/s colorless re-modulation of signal from 1550nm vertical cavity surface emitting laser array in WDM PON," in *Proceedings of Lasers and Electro-Optics (CLEO) and Quantum Electronics and Laser Science Conference* (2009), paper CI3_4.
7. T. B. Gibbon, K. Prince, T. T. Pham, A. Tatarczak, C. Neumeyr, E. Rönneberg, M. Ortsiefer, and I. T. Monroy, "VCSEL transmission at 10Gb/s for 20km single mode fiber WDM-PON without dispersion compensation or injection locking," Opt. Fiber Technol. **17**(1), 41–45 (2011).
8. K. Prince, M. Ma, T. B. Gibbon, C. Neumeyr, E. Rönneberg, M. Ortsiefer, and I. Tafur Monroy, "Free-running 1550 nm VCSEL for 10.7 Gb/s transmission in 99.7 km PON," IEEE/OSA JOCN. **3**, 399–403 (2011).
9. R. Rodes, J. Estaran, B. Li, M. Muller, J. B. Jensen, T. Gruendl, M. Ortsiefer, C. Neumeyr, J. Rosskopf, K. J. Larsen, M.-C. Amann, and I. T. Monroy, "100 Gb/s single VCSEL data transmission link," in *Optical Fiber Communication Conference* (Optical Society of America, 2012), paper PDP5D.
10. E. Hugues-Salas, R. P. Giddings, X. Q. Jin, J. L. Wei, X. Zheng, Y. Hong, C. Shu, and J. M. Tang, "Real-time experimental demonstration of low-cost VCSEL intensity-modulated 11.25 Gb/s optical OFDM signal transmission over 25 km PON systems," Opt. Express **19**(4), 2979–2988 (2011), http://www.opticsinfobase.org/oe/abstract.cfm?URI=oe-19-4-2979.
11. S. C. J. Lee, F. Breyer, S. Randel, J. Zeng, F. Huijskens, H. P. van den Boom, A. M. Koonen, and N. Hanik, "24-Gb/s transmission over 730 m of multimode fiber by direct modulation of an 850-nm VCSEL using discrete multi-tone modulation," in *Optical Fiber Communication Conference* (Optical Society of America, 2009), paper PDP5.

#176871 - $15.00 USD Received 2 Oct 2012; revised 11 Nov 2012; accepted 12 Nov 2012; published 17 Jan 2013

12. K. Szczerba, B.-E. Olsson, P. Westbergh, A. Rhodin, J. S. Gustavsson, A. Haglund, M. Karlsson, A. Larsson, and P. A. Andrekson, "37 Gbps transmission over 200 m of MMF using single cycle subcarrier modulation and a VCSEL with 20 GHz modulation bandwidth," in Proceedings of 36th European Conference on Optical Communication (2010), paper We.7.B.2.
13. J. Proakis and M. Salehi, *Digital Communications* (McGraw-Hill, 2007).
14. J. Justesen, "Performance of product codes and related structures with iterated decoding," IEEE Trans. Commun. **59**(2), 407–415 (2011).

1. Introduction

Vertical cavity surface emitting lasers (VCSELs) have several attractive properties such as large modulation bandwidth, low driving voltage, wavelength tunability, wafer-scale testing, easy packaging, and low carbon footprint [1–4]. These advantages make VCSELs attractive light sources for high-speed optical communication links in data centers and optical access networks using intensity modulation/ direct detection (IM/DD) technique. Optical links that use long-wavelength VCSELs and on-off keying (OOK) modulation are limited in transmission reach by chromatic dispersion of optical fibers due to frequency chirping caused by direct modulation of the VCSEL and large occupied bandwidth of signals [5–8]. For 10-Gbps data transmission using 1.5-μm VCSELs, a 3-dB power penalty after 10-km single mode fiber (SMF) transmission was experimentally observed [6] and a 11-dB power penalty after 20-km SMF was observed after numerical simulations [7]. To deal with the effect of chromatic dispersion for OOK systems, dispersion management and dispersion mitigation methods have been proposed [5–8]. Advanced modulation formats also have been proposed to reduce the bandwidth of the signals. High-speed pulse amplitude modulation (PAM) for VCSELs has been demonstrated [9]. Its scalability is limited because it is single dimension modulation. Multi-tone modulation (DMT), a sub-class of orthogonal frequency division multiplexing (OFDM), is a promising technology for both increasing spectral efficiency and dispersion tolerance. High speed data transmission of DMT signal using VCSELs has been demonstrated recently [10,11]. However, to support high-speed data transmission, DMT requires fast analogue to digital (ADC) and digital to analogue (DAC) converters. Additionally, DMT transceivers consume high power for signal processing compared to conventional OOK transceivers. A simpler method, single-cycle subcarrier quadrature amplitude modulation (QAM) was proposed in which the subcarrier frequency is equal to the symbol rate. Transmission of 10-Gbaud 16-QAM data in a 20-GHz bandwidth over 200-m MMF using 850-nm VCSELs has been reported [12].

In this paper, we analyze and demonstrate sub-cycle QAM modulation for spectrally efficient VCSEL-based optical links. We point out that the subcarrier frequency can be reduced to a quarter or a half of the symbol rate to improve spectral efficiency while the simplicity of the transceiver is maintained. For instance, by using a subcarrier frequency at half the symbol rate, the spectral width, defined as the frequency of the first null in the spectrum, of the QAM signal is reduced by 25% compared to conventional QAM modulation. We demonstrate the generation and detection of 10-Gpbs and 16-Gbps 4-QAM signals transmitted over 20-km and 3-km SMFs respectively using an un-cooled commercially available 10-GHz, 1.5-μm VCSEL. Bit error ratio (BER) below $4.8\text{x}10^{-3}$, the limit of forward error correction (FEC) with 7% payload overhead, was achieved for both cases. 2.5-dB power penalty was observed for 10-Gbps 4-QAM signal after 20-km fiber transmission.

2. Sub-cycle QAM modulation and demodulation

QAM is a two-dimensional signaling method which uses the in-phase and quadrature (cosine and sine waves, respectively). Two basis functions of QAM [13]:

$$\phi_1(t) = \sqrt{\frac{2}{\mathrm{E}_g}} g(t) \cos 2\pi f_c t \tag{1}$$

#176871 - $15.00 USD Received 2 Oct 2012; revised 11 Nov 2012; accepted 12 Nov 2012; published 17 Jan 2013

$$\phi_2(t) = -\sqrt{\frac{2}{\mathrm{E}_g}} g(t) \sin 2\pi f_c t \tag{2}$$

The corresponding signal waveform of M-QAM signals:

$$\begin{aligned} s_m(t) &= A_{mI}\sqrt{\frac{E_g}{2}}\phi_1(t) + A_{mQ}\sqrt{\frac{E_g}{2}}\phi_2(t), \qquad \text{m=1, 2,..., M} \\ &= A_{mI} g(t)\cos 2\pi f_c t - A_{mQ} g(t)\sin 2\pi f_c t \end{aligned} \tag{3}$$

where E_g is the energy of the signal with the lowest amplitude and $g(t)$ is a pulse shape. A_{mI} and A_{mQ} denote the set of M possible amplitudes for I and Q channels. The norms of two basis functions in a symbol duration [0, T]:

$$\begin{aligned} \left\langle \phi_1(t), \phi_1(t) \right\rangle &= \int_0^T \left(\sqrt{\frac{2}{\mathrm{E}_g}} g(t)\cos\left(2\pi f_c t + \varphi\right) \right)^2 \\ &= \int_0^T \frac{2}{\mathrm{E}_g} g^2(t)\cos^2\left(2\pi f_c t + \varphi\right) \end{aligned} \tag{4}$$

$$\begin{aligned} \left\langle \phi_2(t), \phi_2(t) \right\rangle &= \int_0^T \left(\sqrt{\frac{2}{\mathrm{E}_g}} g(t)\sin\left(2\pi f_c t + \varphi\right) \right)^2 \\ &= \int_0^T \frac{2}{\mathrm{E}_g} g^2(t)\sin^2\left(2\pi f_c t + \varphi\right) \end{aligned} \tag{5}$$

The inner product of two basis functions in a symbol duration [0, T]:

$$\begin{aligned} \left\langle \phi_1(t), \phi_2(t) \right\rangle &= \int_0^T \sqrt{\frac{2}{\mathrm{E}_g}} g(t)\cos\left(2\pi f_c t + \varphi\right) \sqrt{\frac{2}{\mathrm{E}_g}} g(t)\sin\left(2\pi f_c t + \varphi\right) \\ &= \int_0^T \frac{2}{\mathrm{E}_g} g^2(t)\sin 2\left(2\pi f_c t + \varphi\right) \end{aligned} \tag{6}$$

The two basis functions are orthogonal if integral of $\sin 4\pi f_c t$ is equal to zero in a symbol duration. We consider the cases subcarrier frequencies are lower than the symbol rate. There are two basic options to achieve that.

2.1. Subcarrier frequency is at half the symbol rate

If the carrier frequency is a half the symbol rate, $fc = \frac{1}{2T}$ (half-cycle modulation), the integral in Eq. (6) is taken in one cycle of $\sin\left(4\pi f_c t\right)$. It is equal to zero regardless the phase of basis functions. The two basis functions for half-cycle QAM modulation:

$$\phi_1(t) = \pm\sqrt{\frac{2}{\mathrm{E}_g}} g(t)\cos\left(2\pi\frac{1}{2T}t + \varphi\right) \qquad \text{t=[0, T]} \tag{7}$$

$$\phi_2(t) = \mp\sqrt{\frac{2}{\mathrm{E}_g}} g(t)\sin\left(2\pi\frac{1}{2T}t + \varphi\right) \qquad \text{t=[0, T]} \tag{8}$$

#176871 - $15.00 USD Received 2 Oct 2012; revised 11 Nov 2012; accepted 12 Nov 2012; published 17 Jan 2013

As in Eqs. (7) and (8), there are two available values for each basis function: positive and negative ones. When full cycle sine/cosine signals are used for data modulation. Those two values of each basis functions are alternately used for two consecutive bits. Nevertheless the two basis functions have unit norm regardless the sign. Therefore, they are an orthonomal set.

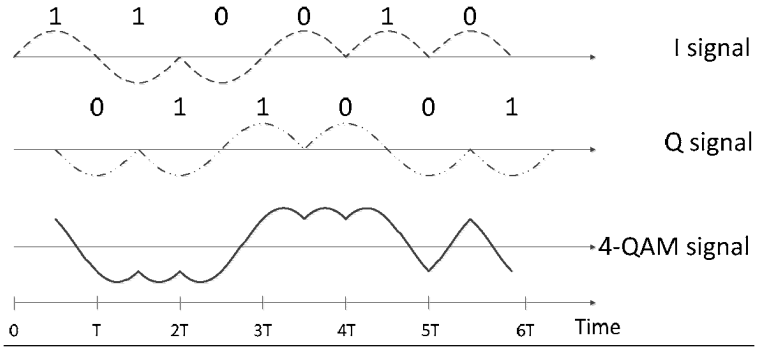

Fig. 1. Simulated waveforms of BPSK signals from I and Q channels and half-cycle 4-QAM signal. There is a half-period offset between the two signal components.

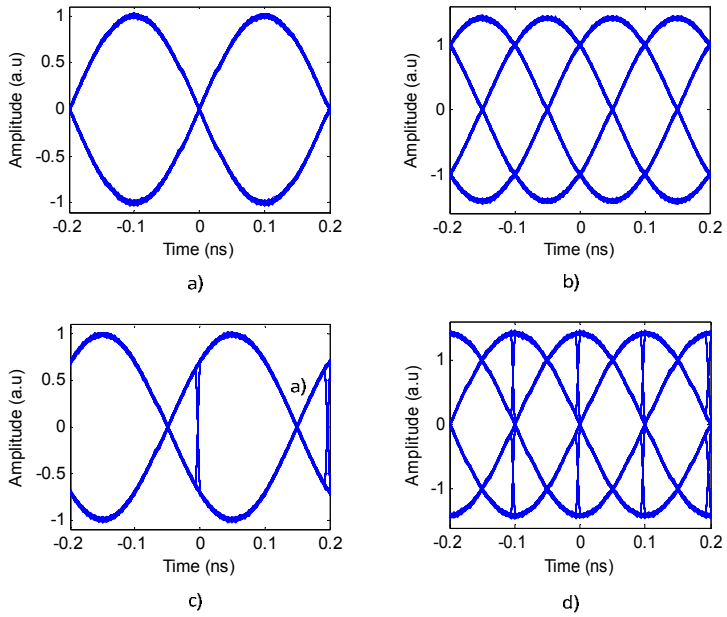

Fig. 2. Simulated eye diagram of 5-Gbaud BPSK signal from I channel and 4-QAM signal in two-baud duration (a,b): data bits start at ± kπ phase of subcarrier, (c,d): data bits start at a different phase.

#176871 - $15.00 USD Received 2 Oct 2012; revised 11 Nov 2012; accepted 12 Nov 2012; published 17 Jan 2013

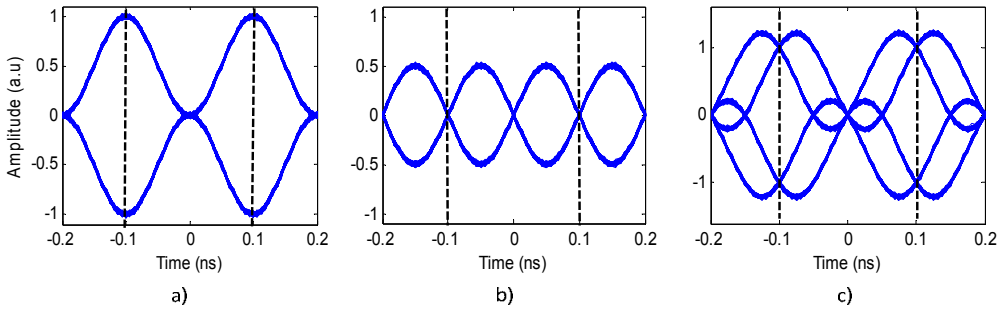

Fig. 3. Simulated eye diagrams of BPSK signal from a) I channel, b) Q channel and c) 4-QAM signal after multiplication with sine signal for detection. Dash lines indicate center of bits - the optimal sampling instant.

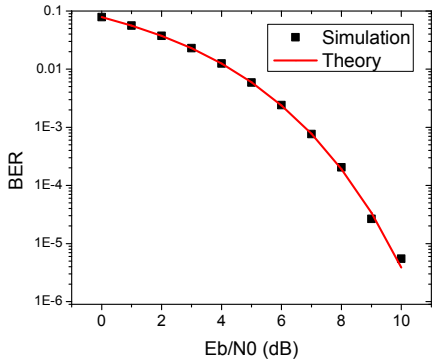

Fig. 4. Theoretical and simulated BER of half-cycle 4-QAM signal in AWGN channel.

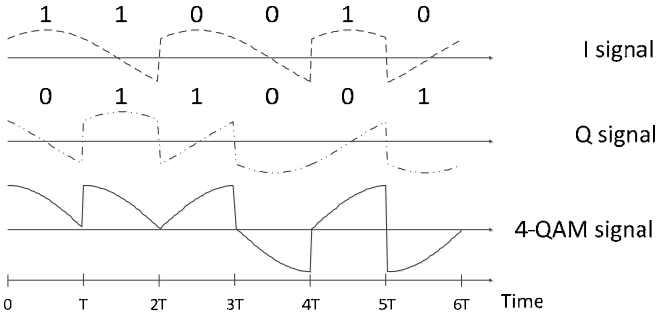

Fig. 5. Simulated waveforms of BPSK signals from I and Q channels and 4-QAM quarter-cycle signal.

#176871 - $15.00 USD Received 2 Oct 2012; revised 11 Nov 2012; accepted 12 Nov 2012; published 17 Jan 2013

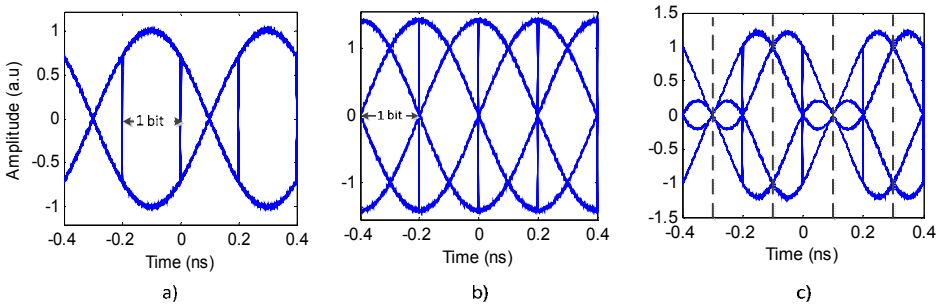

Fig. 6. Simulated eye diagram of 5-Gbaud quarter-cycle modulation signal in 4-baud duration. (a) BPSK signal, (b) 4-QAM signal, (c) 4-QAM signal after multiplication with sine signal. Dash lines indicate center of bits.

Examples of simulated waveforms of the BPSK signals from I and Q channels and half-cycle 4-QAM signal are depicted in Fig. 1. Simulated eye-diagrams of the BPSK signals and the 4-QAM signal are illustrated in Fig. 2. In Figs. 2(a) and 2(b), data bits start when the phase of subcarrier is $\pm k\pi$ (k = 0, 1, 2...) while in Figs. 2(c) and 2(d) data bits start at $\pm \pi/4 + k\pi$ of the subcarrier phase. Data in Q channel is half a bit delayed to make the half-cycle QAM signal consistent with the signal generated in the experiment which is presented in section 3.

The half-cycle QAM signal can be demodulated using a correlation receiver [13]. When multiplied with sine/cosine signals, two values of each basis function are again alternately used. It removes the effect of the sign of the basis functions on the demodulated data. Figure 3 shows the eye-diagrams for two symbols of the BPSK signals from I and Q channels and the 4-QAM signal after multiplication with a sine signal for detection. It shows clearly that the optimal sampling point for threshold gating is at the center of bits when the interference is zero. Therefore, the integration step can be eliminated. The theoretical BER for half-cycle QAM modulation is similar other subcarrier frequencies which is expressed in [13]. The theoretical and simulated BER of the half-cycle 4-QAM signal versus energy-per-bit-to-noise ratio (Eb/N0) in additive white Gaussian noise (AWGN) channel is presented in Fig. 4.

2.2. Subcarrier frequency is at a quarter of the symbol rate

In this case, the integral in Eq. (6) is taken in one half cycle of $\sin(4\pi f_c t)$ starting at $\pm\pi/2$ and ending at $\mp\pi/2$, precisely. It means that data bits must start at $\pm l\pi/2 + \pi/4$ (l = 1,2, ...). The two basis functions for quarter-cycle QAM modulation:

$$\phi_1(t) = \pm\sqrt{\frac{2}{\mathrm{E}_g}}g(t)\cos\left(2\pi\frac{1}{4T}t + \frac{k}{4}\pi\right) \quad \text{t=[0, T], k=1,3} \tag{9}$$

$$\phi_2(t) = \mp\sqrt{\frac{2}{\mathrm{E}_g}}g(t)\sin\left(2\pi\frac{1}{4T}t + \frac{k}{4}\pi\right) \quad \text{t=[0, T], k=1,3} \tag{10}$$

There are four possible values for each basis functions as expressed in Eqs. (9) and (10). However, these four values gives only two different norms. Different norms from different basis functions make the same symbols have different energy levels. Similarly to half-cycle modulation, when full cycle of sine/cosine signal is used for data modulation, all four values are alternately used. Example waveforms of BPSK signals from I and Q channels and quarter-cycle 4-QAM signal are depicted in Fig. 5. Eye-diagrams of the I channel output and the 4-QAM signal are illustrated in Figs. 6(a) and Fig. 6(b). Figure 6(c) represents the eye-diagram of 4-QAM signal after multiplication with the sine signal. As shown in the figure, the interference from the Q channel is zero at the center of the bits. However, the waveforms and

#176871 - $15.00 USD Received 2 Oct 2012; revised 11 Nov 2012; accepted 12 Nov 2012; published 17 Jan 2013

average levels of two consecutive bits are totally different. It means that quarter-cycle modulation not only requires strict phase condition alignment but also a more complicated method for detection.

3. Experimental setup

Due to the strict phase requirement for signal generation and complication of signal detection of quarter-cycle modulation, we chose only half-cycle modulation for the experiment. The experimental setup is illustrated in Fig. 4. There are two important parts in the setup: real time generation and transmission of a half-cycle 4-QAM signal.

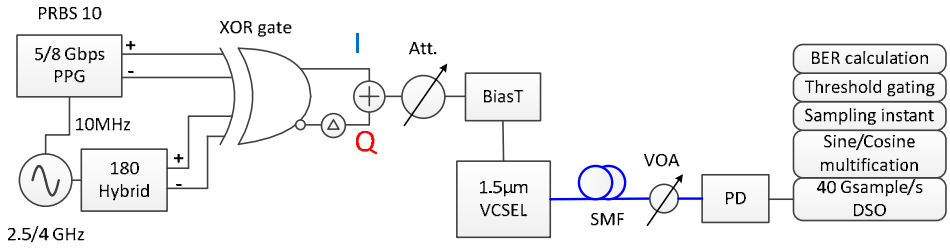

Fig. 7. Experimental setup: Pulse pattern generator (PPG), photodetector (PD), variable optical attenuator (VOA), single mode fiber (SMF), digital storage oscilloscope (DSO).

3.1. Half-cycle 4-QAM signal generation

To generate the electrical half-cycle 4-QAM signal, we used the method proposed in [12]. However, in our case, the subcarrier frequency was equal to half the symbol rate. 2.5/4-GHz subcarrier and synchronized 5/8-Gbps data with PRBS length of 2^{10}-1 were fed to a 13-GHz bandwidth XOR gate (Inphi 13610XR) to create two BPSK signals in the two outputs of the XOR gate. Due to the slow response of the XOR gate, the data bit stream was delayed approximately $\pi/4$ to force the XOR outputs always cross the zero level regardless the input bits. One output of the XOR gate was delayed and then combined with the other one using a power combiner to form a 4-QAM signal. The delay time was optimized in order to secure that the two signals from the XOR outputs are uncorrelated and 90 degrees out of phase. Utilizing a XOR gate to generate half-cycle QAM signals means transmitters of half-cycle QAM signals can be integrated using existing semiconductor process technologies. Compact, low-power transmitters can be produced.

The half-cycle QAM signal has some special features. Firstly, the first null in the spectrum of the signal is at 1.5 times the symbol rate while the first null point of single cycle QAM modulation is at twice the symbol rate. This means that the spectral efficiency of half-cycle QAM modulation is improved by 25% compared to single cycle modulation. The spectra of the generated half-cycle and single-cycle 5-Gbaud 4-QAM signals are illustrated in Fig. 5. It is observed that the width of the first lobe of the half-cycle modulation and the single-cycle modulation is 7.5 and 10 GHz, respectively. In comparison with a OOK signal at the same bit rate, the spectrum of the half-cycle signal has a similar shape to that of the OOK signal but the width of slopes is smaller. For instance, in the case of the 4-QAM signal, the first lobe is 25% less and higher order lobes are 50% less than that of the OOK signal. Secondly, unlike the single-cycle QAM signal, most of the power of the half-cycle QAM signal is concentrated in the low frequency region. This makes the signal more tolerant towards high-frequency roll-off of VCSELs and photodiodes.

3.2. Half-cycle QAM signal transmission

The generated 4-QAM signal was fed to an un-cooled 1.5-μm VCSEL using a BiasT. The threshold current of the VCSEL was 17 mA and it was biased at 22.5 mA for the best performance. With 5-Gbaud data, the optical signal from the VCSEL was transmitted over

#176871 - $15.00 USD Received 2 Oct 2012; revised 11 Nov 2012; accepted 12 Nov 2012; published 17 Jan 2013

20-km standard SMF. The 8-Gbaud signal was transmitted through 3-km SMF. A variable optical attenuator (VOA) was utilized to vary the optical power level into the photodetector (PD). The 3-dB bandwidth of the VCSEL, the evaluation board and the PD was approximately 10 GHz. The photodetected signal was digitized using a 40-GSamples/s digital storage oscilloscope (DSO) for offline digital signal processing (DSP). The DSP algorithm was kept simple without any equalization technique. It includes I/Q detection, optimal sampling, threshold gating and bit error rate (BER) calculation. It indicates that receivers for half-cycle QAM signals can be developed by using the current technologies for receivers of OOK and PAM signals without employing a high-speed ADC.

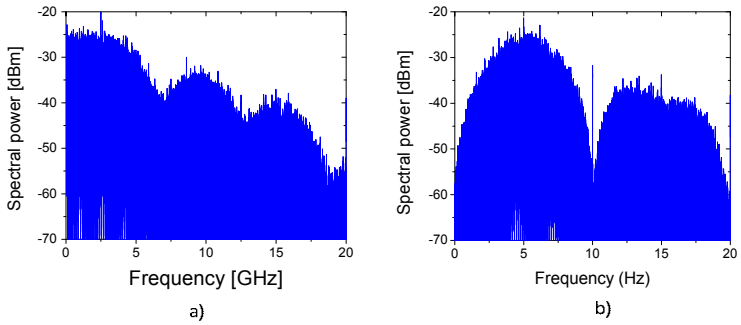

Fig. 8. Spectrum of (a) 5-Gbaud half-cycle 4-QAM signal and (b) 5-Gbaud single-cycle 4-QAM signal.

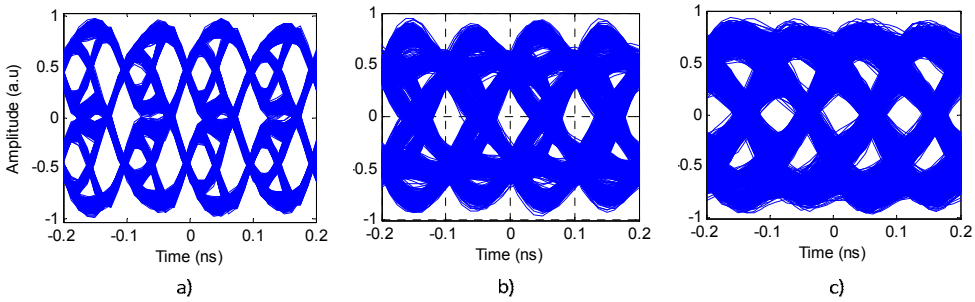

Fig. 9. Eye-diagram of electrical 10-Gbps 4-QAM signal: (a) after XOR gate and after photodetection (b) at B2B and (c) after 20-km SSMF transmission.

4. Experimental results

4.1. Performance of half-cycle QAM signals

The eye-diagrams of the 10-Gbps 4-QAM signals driving the VCSEL, detected signals at B2B and after fiber transmission is illustrated in Fig. 6. To assess the performance of the system, approximately 150k symbols (300k bits) were used to calculate the BER of the signals at both data rates. This number of symbols is limited by BER measurement using offline processing. The lowest detectable BER when there is error is approximately 3.3 10^{-6}. Figure 3 shows the BER of the signals B2B and after fiber transmission. For the 5-Gbaud signal, the optical power to achieve BER of 10^{-5} was about −12 dBm and −10 dBm for B2B and fiber transmission cases, respectively. Assuming that product code with shortened BCH (1023,992) (Bose-Chaudhuri-Hocqenghem) component codes is used and 7% payload is utilized for FEC header, the limit of pre-FEC BER aiming for after- FEC BER of 10^{-15} is $4.8\text{x}10^{-3}$ [14]. At this FEC limit, the receiver sensitivity B2B was approximately −15 dBm and the power penalty after 20-km SSMF transmission was only 2.5 dB.

#176871 - $15.00 USD Received 2 Oct 2012; revised 11 Nov 2012; accepted 12 Nov 2012; published 17 Jan 2013

For the 8-Gbaud signal B2B, as shown in Fig. 3(b), the receiver sensitivity at BER of 10^{-5} was about −6.7 dBm and at the FEC limit was −11.0 dBm. Due to the increased signal bandwidth and the strong effect of jitter after fiber transmission, the 8-Gbaud signal has higher transmission power penalty than the 5-Gbaud signal. After 3-km SMF, the power penalty was approximately 1.5 dB. In general, the receiver sensitivity was approximately 5 dB worse than for the 5-Gbaud signal. This performance limitation are attributed the imperfection of the generated QAM signal before modulation and limited bandwidth of the transceivers. The generated 8-Gbaud signal had lower signal-to-noise ratio (SNR) than the 5-Gbaud signal and the bandwidth of the 8-Gbaud signal was 12 GHz. Examples of the constellations of both 5-Gbaud and 8-Gbaud signals before modulating the VCSEL and at B2B are presented in Fig. 8 and Fig. 9.

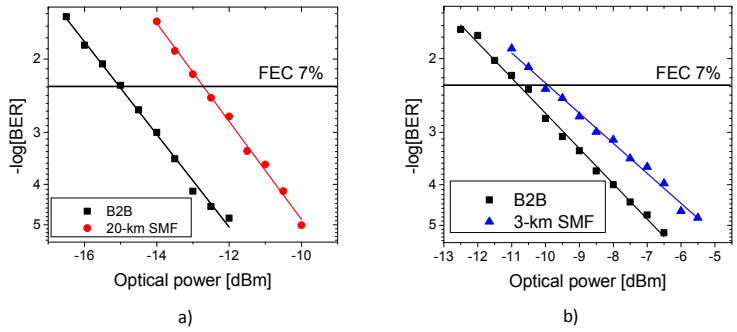

Fig. 10. Performance of 4-QAM signals at B2B and after fiber transmission: (a) 5 Gbaud (10Gbps) and (b) 8 Gbaud (16 Gbps).

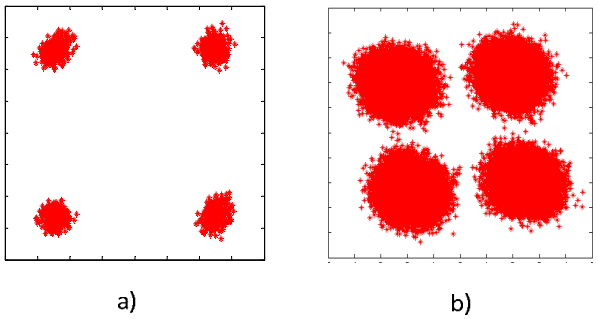

Fig. 11. Constellation of 5-Gbaud 4-QAM signal: (a) generated electrical signal and (b) at −12.0 dBm B2B.

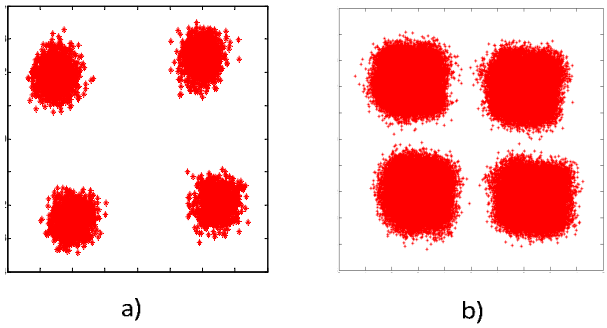

Fig. 12. Constellation of 8-Gbaud 4-QAM signal: (a) generated electrical signal and (b) at −6.5 dBm B2B.

#176871 - $15.00 USD Received 2 Oct 2012; revised 11 Nov 2012; accepted 12 Nov 2012; published 17 Jan 2013

4.2. Comparison with OOK signal

In this section, we compare the performance of our proposed half-cycle QAM signal with the conventional OOK signals. Two data rates of 5 Gbps and 10 Gbps with direct current (DC) removed were chosen for the comparison with 5-Gbaud 4-QAM signal. The 5-Gbps OOK signal has the same baudrate while the 10-Gbps signal has the same data rate to the half-cycle QAM signal. The peak-to-peak voltage (V_{p-p}) of OOK signal driving the VCSEL was chosen to be equal to the V_{p-p} of the half-cycle QAM signals at the optimal sampling points as shown in Fig. 2(a). No other conditions of the experiment were changed. The performance of OOK signals at B2B and after 20-km fiber transmission is illustrated in Fig. 4.

At the FEC limit, the sensitivity of the QAM signal was approximately 2 dB and 1.5 dB lower than that of 5-Gbps and 10-Gbps OOK signal because the QAM signal has lower signal-to-noise ratio (SNR). The power penalty after 20-km fiber transmission of 5-Gbps OOK signal was only 1 dB but power penalty of 10-Gbps signal was about 3-dB at FEC limit and increased up to 5-dB at BER of 10^{-5}. It means that the half-cycle QAM signal has improved the dispersion tolerance by only 0.5 dB at FEC limit but it increases dramatically at lower BER. At BER of 10^{-5}, 2.5-dB improvement has been observed.

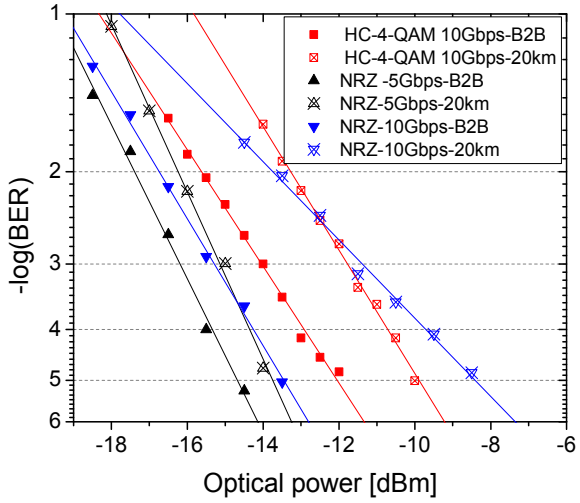

Fig. 13. Performance of 5-Gpbs and 10-Gbps NRZ signals at B2B and after fiber transmission in comparison with 10-Gbps half-cycle 4-QAM signal.

6. Conclusions

We have investigated QAM modulation utilizing sub-cycle subcarrier for VCSEL-based optical links to improve spectral efficiency. The transmission of 10-Gbps 4-QAM data in 7.5-GHz electrical bandwidth over 20-km single mode fiber was demonstrated with BER below the FEC limit and only 2.5-dB power penalty. Half-cycle signals have superior dispersion tolerance compared to OOK signals at the same data rate. Spectral efficiency can be improved by increasing the levels of the QAM signal. Both the transmitter and the receiver can be implemented using available electronics. Half-cycle subcarrier QAM modulation has potential for applications in high-speed PON networks as well as high-performance data centers.

#176871 - $15.00 USD Received 2 Oct 2012; revised 11 Nov 2012; accepted 12 Nov 2012; published 17 Jan 2013